

## Supporting Information

### **Tuning the ultrasonic and photoacoustic response of polydopamine-stabilized perfluorocarbon contrast agents**

Yijun Xie<sup>‡,a,b</sup>, Junxin Wang<sup>‡,c</sup>, James Wang<sup>c</sup>, Ziyang Hu<sup>d</sup>, Ali Hariri<sup>c</sup>, Nicholas Tu<sup>a</sup>, Kelsey A. Krug<sup>a</sup>, Michael D. Burkart<sup>a</sup>, Nathan C. Gianneschi<sup>d</sup>, Jesse V. Jokerst<sup>\*,c</sup>, and Jeffrey D. Rinehart<sup>\*,a,b</sup>

<sup>a</sup>Department of Chemistry and Biochemistry, University of California, San Diego, La Jolla, CA 92093, USA

<sup>b</sup>Materials Science and Engineering Program, University of California, San Diego, La Jolla, CA 92093, USA

<sup>c</sup>Department of NanoEngineering, University of California, San Diego, La Jolla, CA 92093, USA

<sup>d</sup>Department of Chemistry, Northwestern University, Evanston, IL 60208, USA

<sup>‡</sup> Authors contributed equally to the work.

#### **Corresponding author**

\*Email: [jrinehart@ucsd.edu](mailto:jrinehart@ucsd.edu)  
[jjokerst@eng.ucsd.edu](mailto:jjokerst@eng.ucsd.edu)

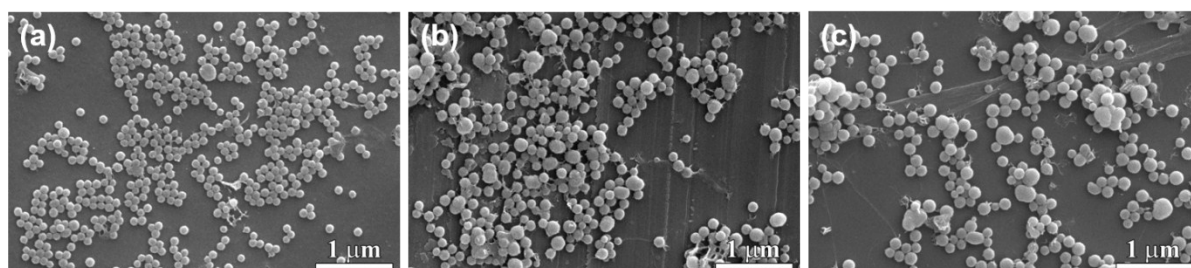


**Figure S1.** SEM images for (a) PDAF-0.13%, (b) PDAF-1.0%, (c) PDAF-1.7%.

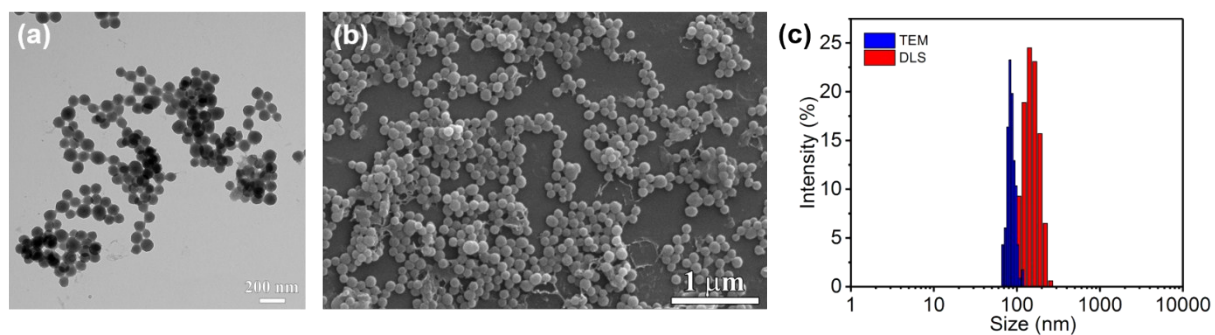


**Figure S2.** Comparison of structural data for a representative sample of PDAF NPs doped to 0.14% Fe ion content by ICP-MS analysis with 6 mg of initial  $\text{FeCl}_3$  loading amount. (a) TEM, (b) SEM, and (c) comparative analysis of diameters determined by TEM and DLS.

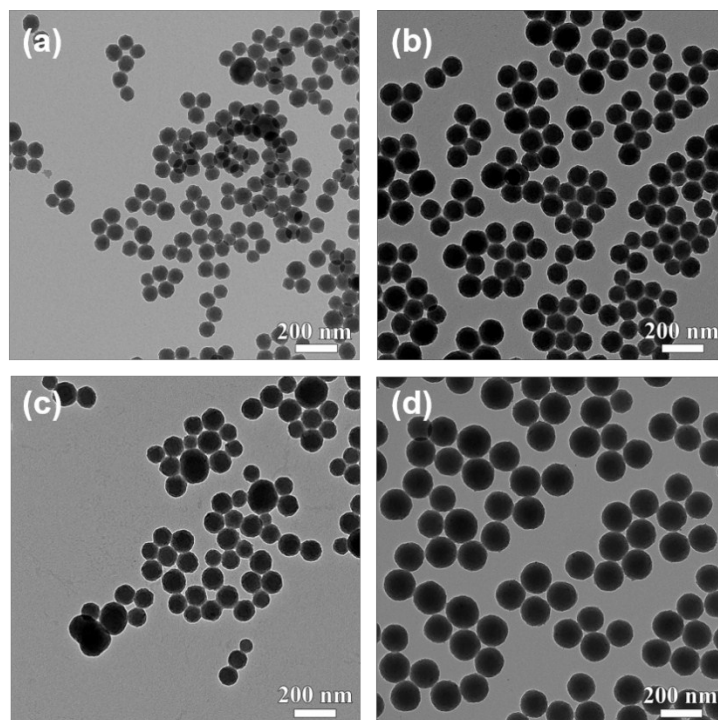


**Figure S3.** TEM images for (a) PDA-Fe-0.13%, (b) PDA-Fe-1.0%, (c) PDA-Fe-1.7%, (d) PDA-Fe-2.4%.

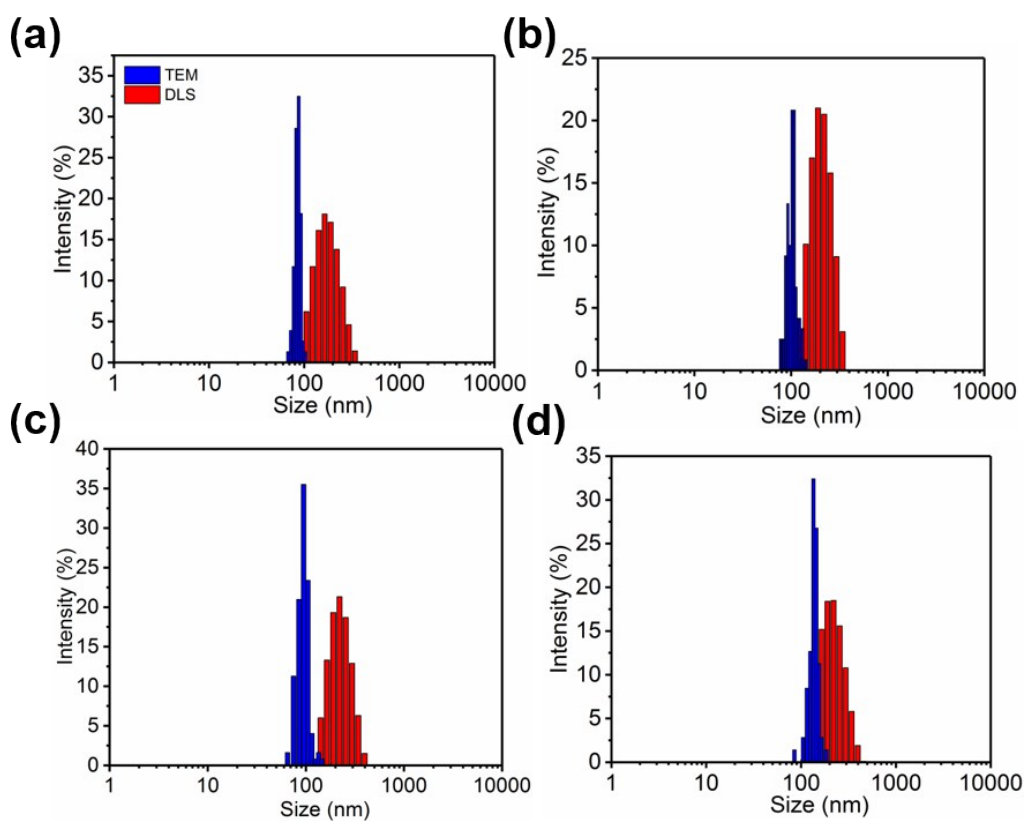


**Figure S4.** Comparison between the particle and hydrodynamic diameters as measured by TEM and DLS for (a) PDAF-0.13%, (b) PDAF-1.0%, (c) PDAF-1.7%, (d) PDAF-2.4%.

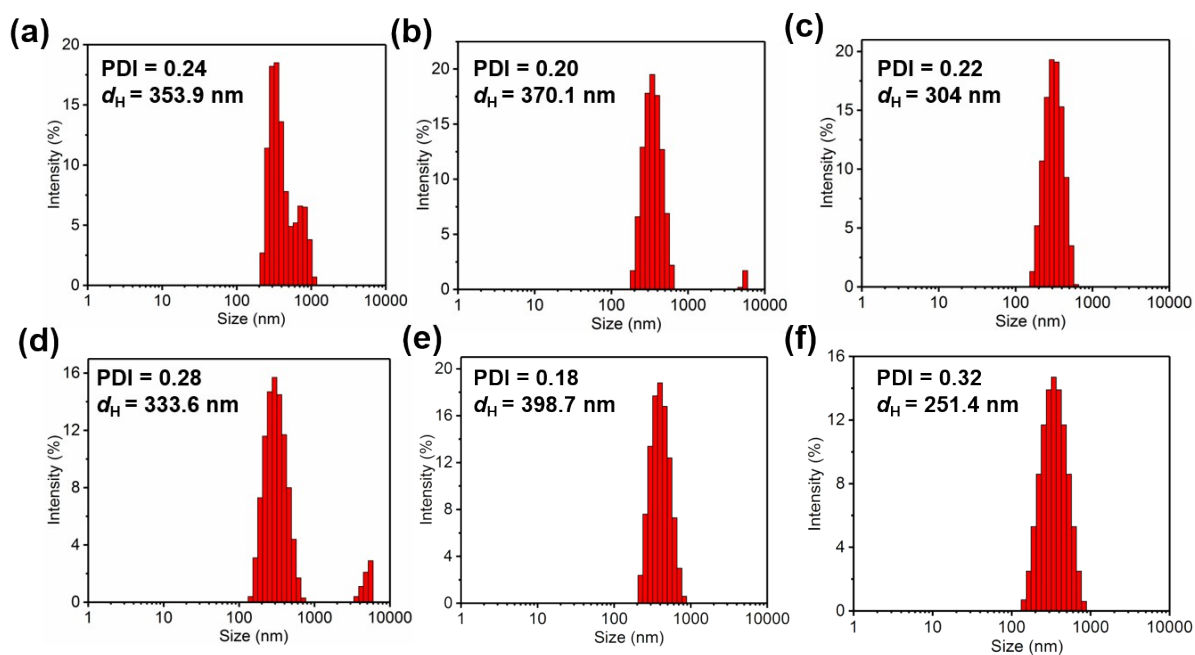


**Figure S5.** DLS size distributions of PFP-loaded (a) PDAF-0.13%, (b) PDAF-1.0%, (c) PDAF-1.7%, (d) PDAF-2.4% in water; DLS size distributions of PFP-loaded PDAF-2.4% in (e) PBS and (f) FBS.

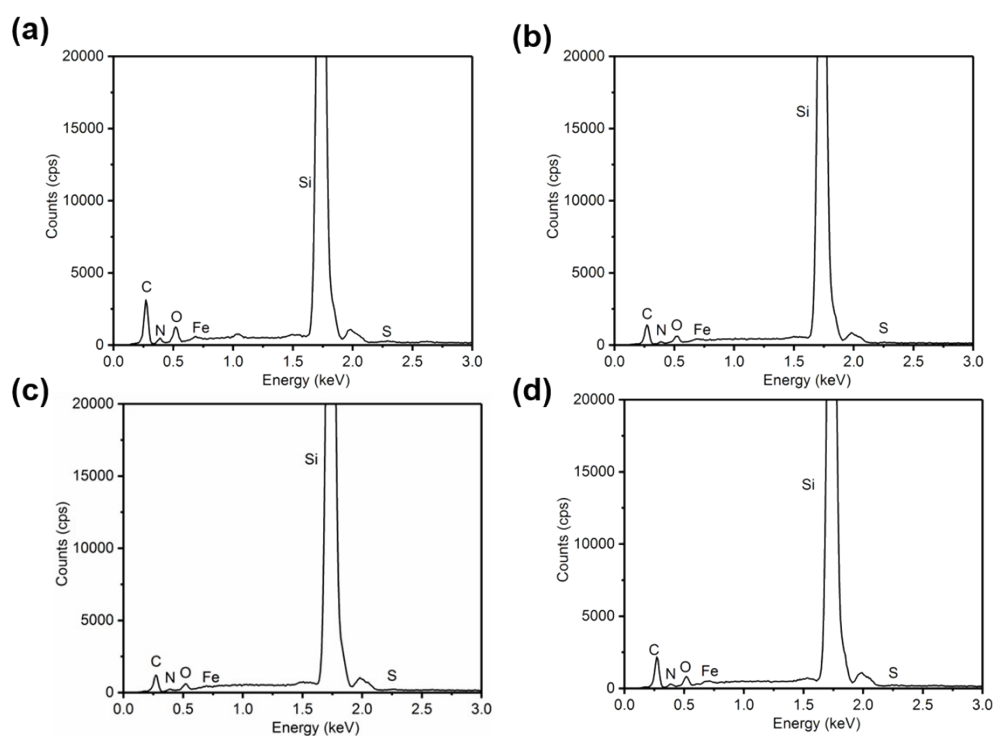


**Figure S6.** EDS spectrum of (a) PDAF-0.13%, (b) PDAF-1.0%, (c) PDAF-1.7%, (d) PDAF-2.4%.

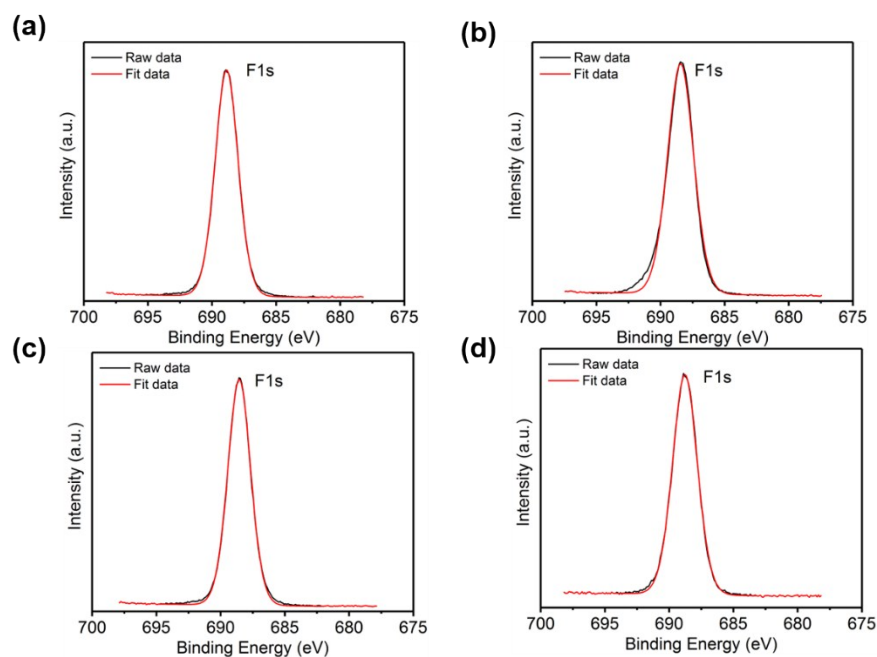


**Figure S7.** F1s XPS spectra of (a) PDAF-0.13%, (b) PDAF-1.0%, (c) PDAF-1.7%, (d) PDAF-2.4%.

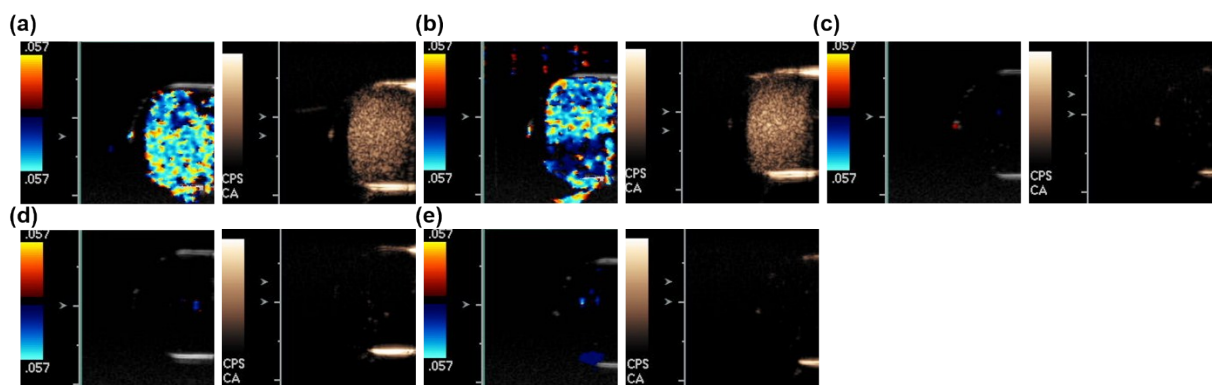


**Figure S8.** Color Doppler and CPS imaging of PFP-loaded (a) PDAF-1.0 %, (b) PDAF-1.7%, (c) PDA-Fe-0.13%, (d) PDA-Fe-1.0%, and (e) PDA-Fe-1.7% at room temperature with MI=1.9.

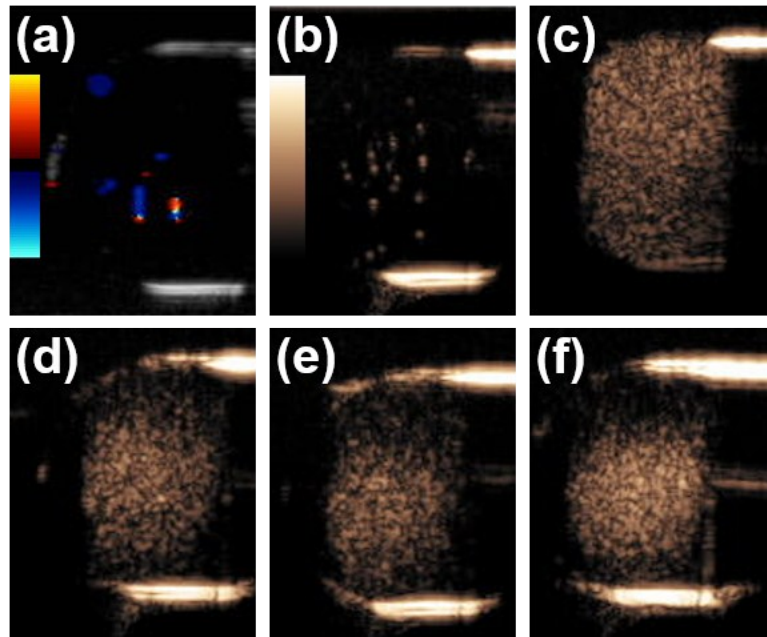


**Figure S9.** (a) Color Doppler, (b) CPS imaging of PFP-water mixtures at room temperature with  $MI = 1.9$ ; CPS imaging of PFP-loaded (c) PDAF-0.13 %, (d) PDAF-1.0 %, (e) PDAF-1.7 %, and (f) PDAF-2.4 % with  $MI = 1.2$ .

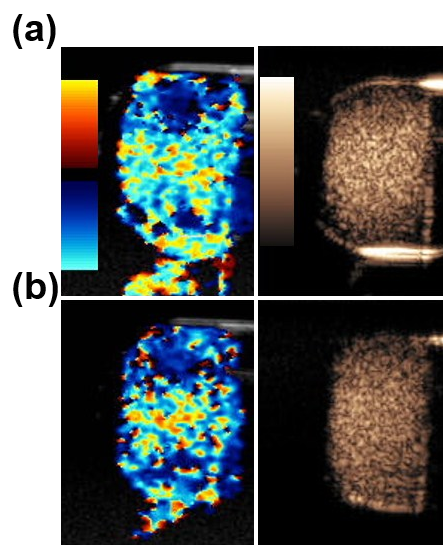


**Figure S10.** Color Doppler and CPS imaging of (a) PFH-loaded, (b) PFB-loaded PDAF-2.4% NPs at 7 MHz at room temperature with  $MI=1.9$ .

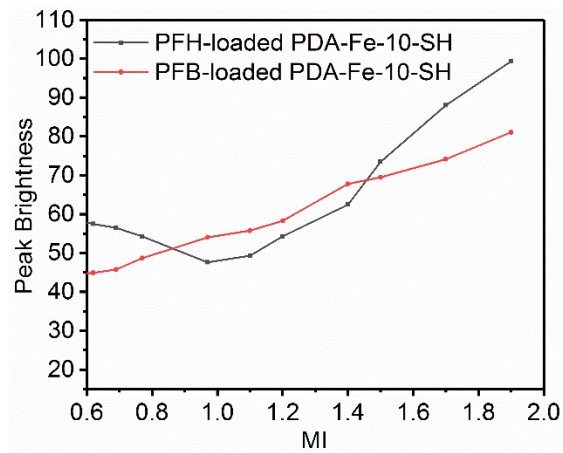


**Figure S11.** Quantitative plot of brightness for CPS imaging of PFH-loaded and PFB-loaded PDAF-2.4% NPs at room temperature.

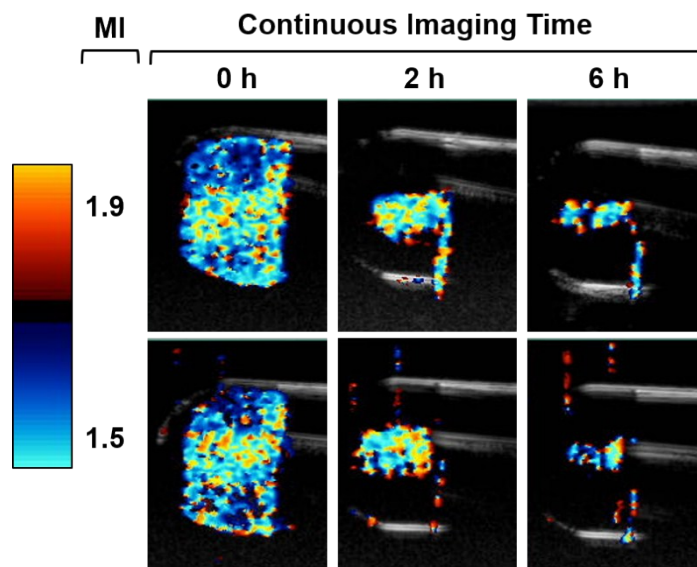


**Figure S12.** Continuous color Doppler imaging of PDAF-2.4% detected at room temperature with MI=1.9 and MI=1.5.

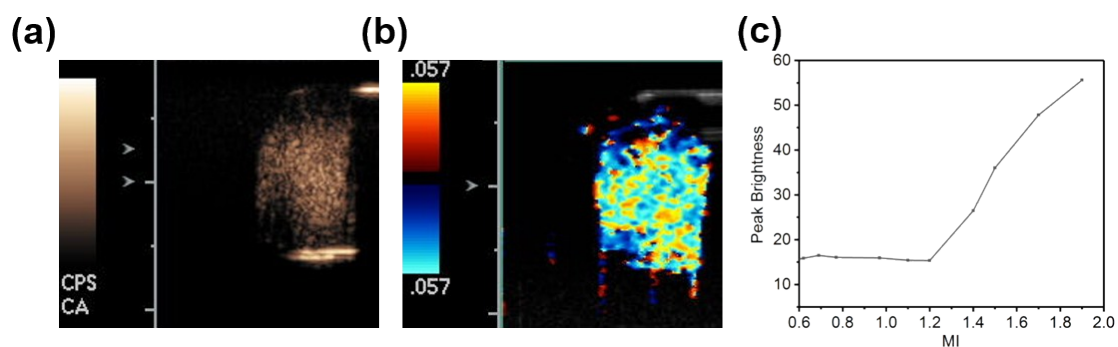


**Figure S13.** 50-day storage lifetime test of PDAF-2.4% NPs using (a) CPS imaging, (b) color Doppler imaging, and (c) quantitative analysis of brightness for CPS imaging versus MI.

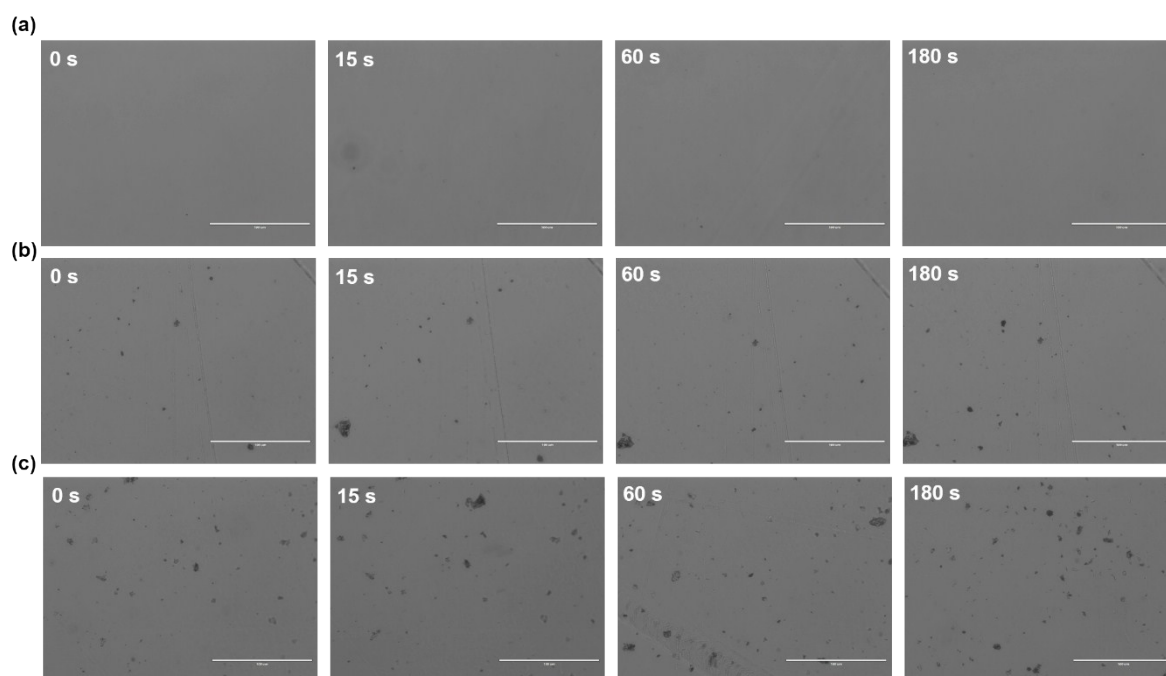


**Figure S14.** Optical microscope images of PFP-loaded (a) PDAF-small, (b) PDAF-large, and (c) PDAF-mix under 5 MHz ultrasound for different time. Scale bar represents 100  $\mu\text{m}$ .

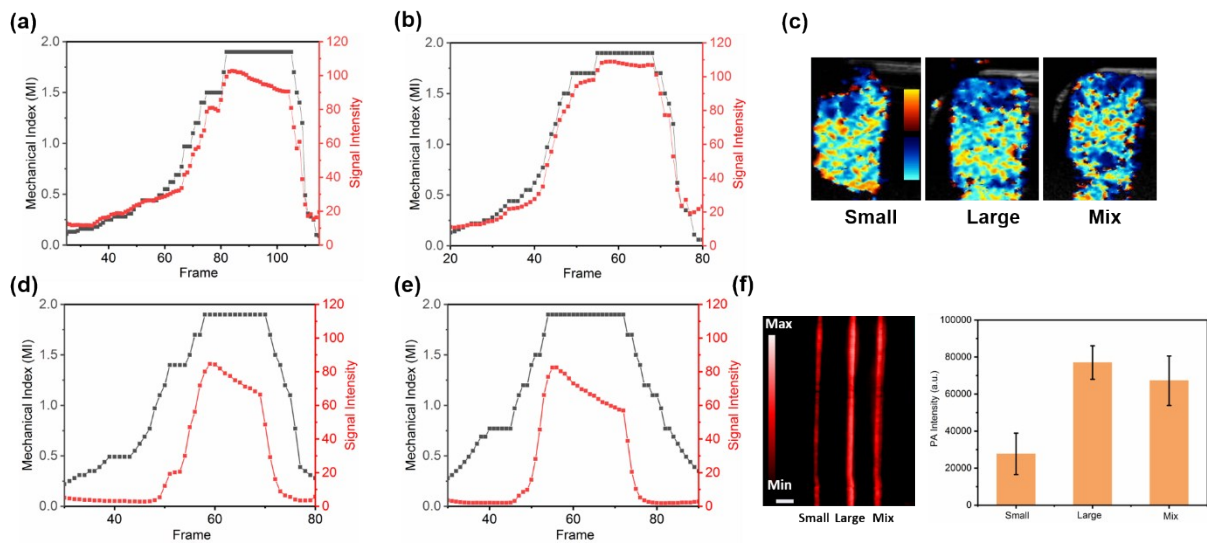


**Figure S15.** Quantitative analysis of image signal intensity and MI versus frame number for CPS imaging of PFP-loaded (a) PDAF-large, and (b) PDAF-mix. (c) Corresponding color Doppler images for PDAF-small, PDAF-large, and PDAF-mix. Quantitative analysis of (d) second, (e) third cycle of CPS imaging for PDAF-small particles (Figure 5f is the first cycle). (f) PA imaging of PFP-loaded PDAF-small, PDAF-large, and PDAF-mix, and their quantitative analysis of PA signal. Scale bar = 3 mm.

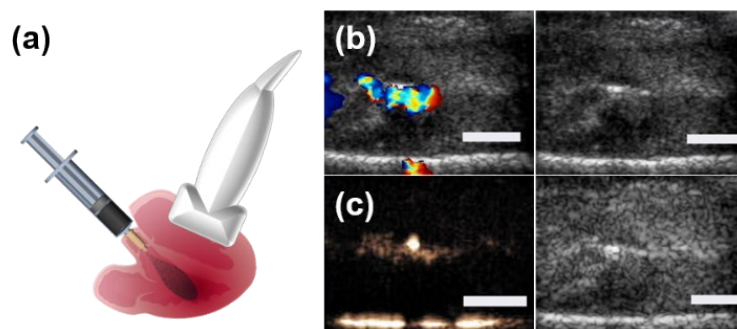


**Figure S16.** Representative data for chicken heart *Ex vivo* tissue experiments. (a) Schematic illustration of the imaging geometry and method for introducing contrast agent to the left ventricle and imaging through (b) Color Doppler and (c) CPS modes with PDAF-2.4% NPs.

The black and white images at right are the underlying B-mode signal. The scale bar in panel (b) and (c) is 5 mm.

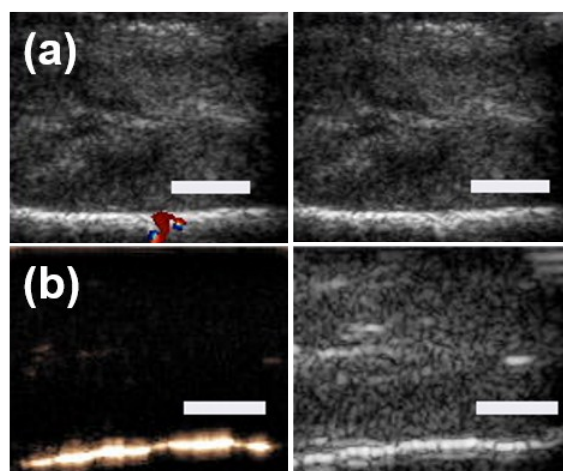


**Figure S17.** *Ex vivo* US imaging of deionized water in the left ventricle imaged through cardiac tissue of a chicken heart. The bright line at the bottom of (b) is an artifact. The scale bar in panel (b) and (c) is 5 mm.

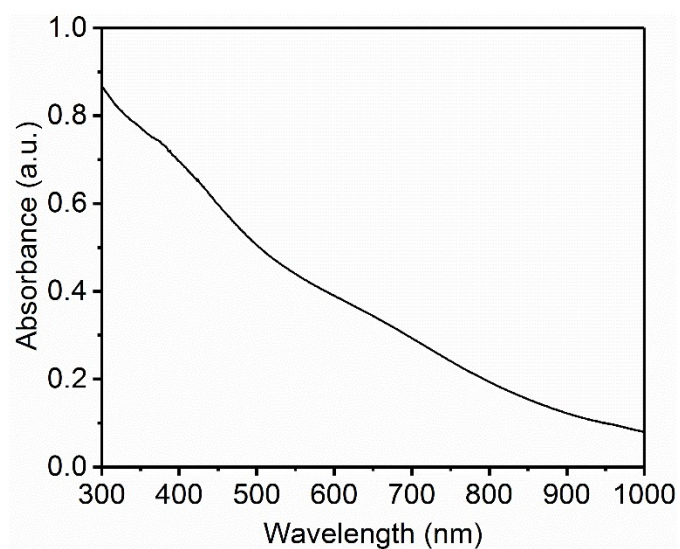


**Figure S18.** UV-vis spectrum of PDAF-2.4%.



**Figure S19.** Experimental setup for *ex vivo* PA imaging.

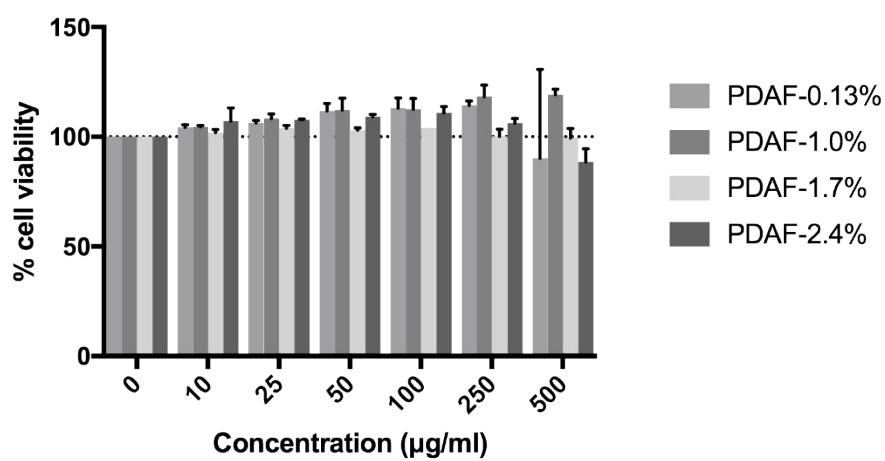


**Figure S20.** Cell viability of HCT116 cells after incubation with the concentration of PDAF-0.13%, PDAF-1.0%, PDAF-1.7%, and PDAF-2.4% increase from 0-500 µg/mL for 24 h.

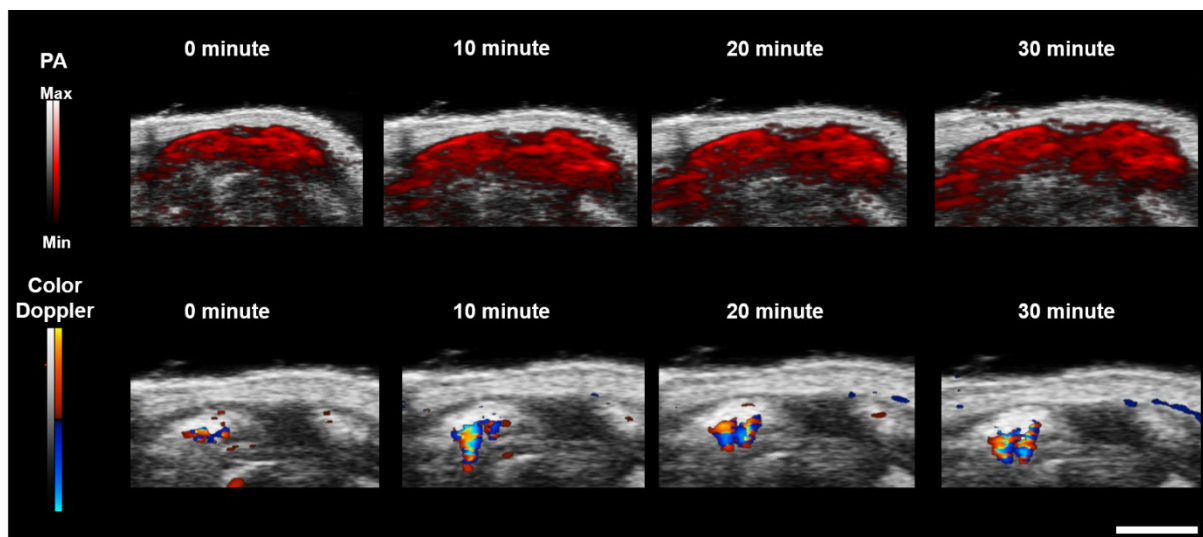


**Figure S21.** Time dependence of PA and color Doppler imaging from initial injection (0 min) to 30 min using PFH-loaded PDAF-2.4%. Scale bar represents 2 mm.

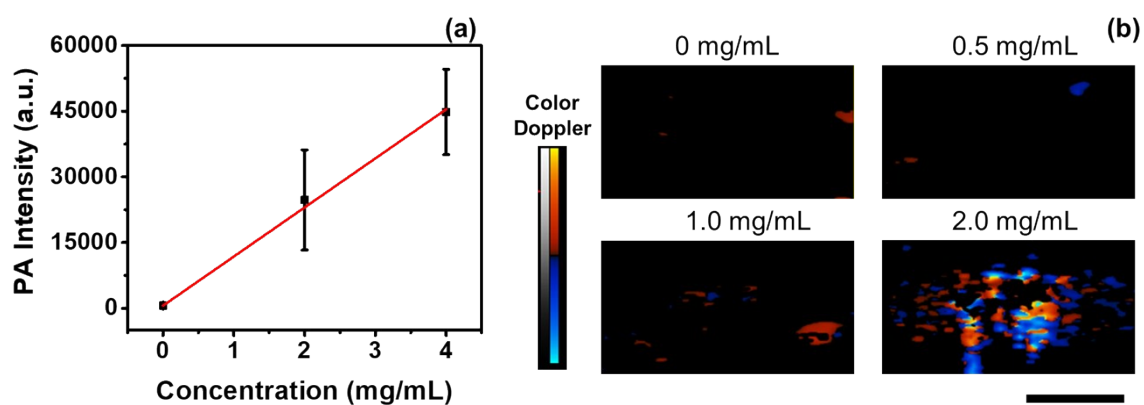


**Figure S22.** The detection limit of the subcutaneous injected PDA-PFH NPs is (a) 0.12 mg/mL (3 standard deviation above the average of baseline) for photoacoustic signal and (b) around 2.0 mg/mL for the color Doppler signal. Error bars in (a) represent standard deviation of 6 regions of interest. Scale bar represents 2 mm.